

Published in final edited form as:

*Int J Radiat Oncol Biol Phys.* 2011 January 1; 79(1): 10–18. doi:10.1016/j.ijrobp.2009.10.058.

## Development and validation of a heart atlas to study cardiac exposure to radiation following treatment for breast cancer

Mary Feng, M.D.<sup>1</sup>, Jean M. Moran, Ph.D.<sup>1</sup>, Todd Koelling, M.D.<sup>2</sup>, Amer Chughtai, M.D.<sup>3</sup>, June L. Chan, M.D.<sup>1</sup>, Laura Freedman, M.D.<sup>1</sup>, James A. Hayman, M.D.<sup>1</sup>, Reshma Jagsi, M.D., D. Phil.<sup>1</sup>, Shruti Jolly, M.D.<sup>1</sup>, Janice Larouere, M.D.<sup>1</sup>, Julie Soriano, M.D.<sup>1</sup>, Robin Marsh, C.M.D.<sup>1</sup>, and Lori J. Pierce, M.D.<sup>1</sup>

<sup>1</sup> Department of Radiation Oncology, University of Michigan Medical Center

<sup>2</sup> Department of Internal Medicine, Division of Cardiology, University of Michigan Medical Center

<sup>3</sup> Department of Radiology, University of Michigan Medical Center

### Abstract

**Purpose**—Cardiac toxicity is an important sequela of breast radiotherapy. However, the relationship between dose to cardiac structures and subsequent toxicity has not been well defined, partially due to variation in substructure delineation, which can lead to inconsistent dose reporting and the failure to detect potential correlations. Here we have developed a heart atlas and evaluated its effect on contour accuracy and concordance.

**Methods and Materials**—A detailed cardiac CT atlas was developed jointly by cardiology, cardiac radiology, and radiation oncology. Seven radiation oncologists were recruited to delineate the whole heart (WH), left main (LM), left anterior descending interventricular branch (LAD), and right coronary arteries (RCA) on four cases before and after studying the atlas. Contour accuracy was assessed by percent overlap with gold standard (GS) atlas volumes. The concordance index (CI) was also calculated. Standard radiation fields were applied. Doses to observer-contoured cardiac (OC) structures were calculated, and compared with GS contour doses. Pre- and post- atlas values were analyzed using a paired t-test.

**Results**—The cardiac atlas significantly improved contour accuracy and concordance. Percent overlap and CI of OC and GS volumes improved for all structures, by up to 2.3-fold ( $p < 0.002$ ). After application of the atlas, reported WH, LM, LAD, and RCA mean doses were within 0.1, 0.9, 2.6, and 0.6 Gy of GS doses.

**Conclusions**—This validated University of Michigan cardiac atlas may serve as a useful tool in future studies assessing cardiac toxicity and in clinical trials which include dose volume constraints to the heart.

---

Please address correspondence to: Mary Feng, Department of Radiation Oncology, University of Michigan Medical Center, 1500 East Medical Center Drive, UH B2C490 SPC 5010, Ann Arbor, MI 48109. Phone: 734-936-4288. Fax: 734-763-7370. maryfeng@umich.edu.

Presented in part at the Multidisciplinary Breast Cancer Symposium, Washington, DC, Sept 5–7, 2008.

#### Conflicts of Interest Notification

No actual or potential conflicts of interest exist.

**Publisher's Disclaimer:** This is a PDF file of an unedited manuscript that has been accepted for publication. As a service to our customers we are providing this early version of the manuscript. The manuscript will undergo copyediting, typesetting, and review of the resulting proof before it is published in its final citable form. Please note that during the production process errors may be discovered which could affect the content, and all legal disclaimers that apply to the journal pertain.

## Keywords

cardiac dysfunction; breast cancer; thoracic radiotherapy; cardiac atlas; normal tissue sparing

---

## INTRODUCTION

Adjuvant radiotherapy is a standard component of breast cancer treatment, both in women undergoing breast conservation therapy, as well as in patients at high risk for local-regional recurrence following mastectomy. With improved therapies, patients are often cured and survive long enough for long-term effects to become apparent. In the past several years, cardiac toxicity has been recognized as an important sequela of breast radiotherapy, particularly among patients treated for left-sided disease.<sup>1–3</sup> Although investigators have found statistical correlations between patients who received breast radiotherapy and later developed cardiac disease, the specific relationships between doses to cardiac structures and subsequent toxicity have not been well defined, likely due in large part to variation in structure delineation. This can lead to inconsistent reporting of doses and the failure to detect potential dose-volume correlations. In the era of systemic therapies including anthracyclines and trastuzumab, which carry an independent risk of cardiac toxicity, any additional potential risk due to radiotherapy must be identified and kept to a minimum.

As a first step, we have developed a heart atlas and evaluated its effect on contour accuracy and concordance. We have included substructures including vessels, chambers, valves, and the conduction system to allow for substructure identification and dose estimation in future studies.

## METHODS AND MATERIALS

### Development of cardiac atlas

A detailed cardiac CT atlas was developed jointly by a cardiologist (T.K.), cardiac radiologist (A.C.), and radiation oncologist (M.F.). Images were obtained with respiratory gating, with and without intravenous contrast. The whole heart was delineated, along with sub-structures including the chambers, great vessels, cardiac valves, conduction system, and major coronary vessels. The contours were agreed upon by all three investigators and were considered to be the gold standard (GS) volumes for future reference. Written guidelines for consistent delineation, as noted below, were also jointly developed.

### Validation of cardiac atlas

Seven radiation oncologists from the University of Michigan Health System who routinely treat breast cancer were recruited for this study. Two specialize in breast cancer treatment at the main hospital, and five treat multiple disease sites, including breast cancer, at affiliate clinics. A pre- and post-test study was designed using breath hold CT scans obtained on four patients with left-sided breast cancer, using active breathing control (ABC), as part of an institutional review board approved study. Patients were positioned supine, on a breast board, with both arms raised above their heads. Radio-opaque catheters were placed at the inferior portion of the clavicular head and midline. For breast conservation cases, catheters were also placed 1.5 cm inferior and lateral to breast tissue, but no further posterior than the mid-axillary line. For post-mastectomy cases, catheters were placed in similar positions based on the position of the contralateral breast. Breathing was suspended at 80% of deep inhalation, and CT images with and without intravenous contrast were obtained. Four sets of images, 2 with intravenous contrast and 2 without, were selected to represent the range of heart positions relative to the chest wall. Images were imported into our in-house treatment

planning system, UMPLAN. On each of the 4 cases, observers contoured the whole heart (WH), left main (LM), left anterior descending interventricular branch (LAD), and right coronary arteries (RCA) before and after studying the atlas. On the scans with IV contrast, observers also contoured the left and right ventricles. All contours were stored separately, so no observers had access to their previous contours or those of their peers. As previously noted, GS contours were generated by the primary investigator upon consultation and review by physicians from Cardiology and Cardiac Radiology.

Contour accuracy was assessed by percent overlap of observer volumes with GS volumes and the concordance index (CI), which was defined as the intersection of observer and gold standard volumes divided by the union of these volumes. A value of 1 indicates perfect concordance. To evaluate the dosimetric impact of potential changes in structure delineation, standard fields were applied to the CT scans to cover the breast tissue and regional nodes including the supraclavicular, infraclavicular, and internal mammary nodes in interspaces 1–3. The pre-placed radio-opaque catheters were used as a guide to design beams for 3-dimensional dosimetric plans. The intact breast cases were planned with 6MV partially-wide tangential fields and a supraclavicular field to a dose of 50 Gy. In addition to tangential and supraclavicular fields, the chest wall cases required a 9MEV medial electron field to encompass internal mammary nodes in interspaces 1 thorough 3. The medial electron field is routinely used in our clinics if the heart is deemed too anterior to allow for partial-wide tangential fields. All fields delivered 50 Gy to the plan normalization point. Dose volume histograms were generated for all contoured structures. Doses to observer-contoured cardiac structures were calculated and compared with GS contour doses using the following formula:

$$\frac{\text{Dose to observer contour} - \text{Dose to gold standard contour}}{\text{Dose to gold standard contour}}$$

All comparisons were evaluated using a 2-sided paired t-test, with  $p < 0.05$  indicating a significant difference.

## RESULTS

### Cardiac atlas

A detailed cardiac atlas consisting of images, with and without intravenous contrast, and written instructions describing the anatomy, were provided (Figures 1 and 2). For optimal visualization of most structures on CT images, a level of 50 and window of 500 was recommended. For viewing cardiac vessels, a level of 50 and window of 150 was suggested.

**Whole Heart and Pericardium**—Superiorly, the whole heart starts just inferior to the left pulmonary artery. For simplification, a round structure to include the great vessels as well can be contoured. Inferiorly, the heart blends with the diaphragm. Since cardiac vessels run in the fatty tissue within the pericardium, this should be included in the contours, even if there is no heart muscle visible in that area. If contrast is administered, the superior vena cava (SVC) can generally be separately contoured from the whole heart. If this is not possible, or it is a non-contrast scan, the SVC can be included for simplification and consistency.

### Chambers

1. The left atrium is typically the most superior chamber on axial CT. It is located to the left and posterior to the pulmonary trunk, and begins just inferior to the left pulmonary artery.
2. The left ventricle is typically anterior and to the left of the left atrium.
3. The right atrium starts to the right of the aortic root superiorly. It moves significantly, so the size of the chamber often appears to change size from slice to slice on a non-cardiac-gated CT.
4. The right ventricle lies directly beneath the sternum and connects to the pulmonary trunk.

### Vessels

1. The left main coronary artery originates from the left side of the ascending aorta, inferior to the right pulmonary artery.
2. The left anterior descending artery, interventricular branch, originates from the left coronary artery, and runs in the interventricular groove, between the right and left ventricles. If it is difficult to see, raising the level and lowering the window may help (e.g. level 50, window 150).
3. The left circumflex artery originates from the left coronary artery, and runs between the left atrium and ventricle. This moves significantly with cardiac motion, so often the location can seem discontinuous from axial CT slice to slice, as the position of the AV groove changes.
4. The right coronary artery originates from the right side of the ascending aorta. Due to the native heart position in the chest, on axial CT, it appears to start inferior to the left coronary artery. It moves significantly with cardiac motion, so often the location can seem discontinuous from axial CT slice to slice, as the position of the AV groove changes.

### Valves

1. The aortic valve is found within the ascending aorta and seen in cross-section on axial CT. In a contrast scan, the leaflets typically create a “Y” within the lumen of the vessel
2. The pulmonic valve is found within the pulmonary trunk and seen in cross-section on axial CT. In a contrast scan, the leaflets typically create an “X” within the lumen of the vessel.
3. The tricuspid valve is located between the right atrium and ventricle. It is difficult to see, but it is defined as the area where the blood pool between the atrium and ventricle is shared. Due to cardiac motion, this can appear to be discontinuous from axial CT slice to slice.
4. The mitral valve is located between the left atrium and ventricle. It is difficult to see, but it is defined as the area where the blood pool between the atrium and ventricle is shared.

**Conduction system**—The AV node cannot be seen on CT, since it has the same signal intensity as the surrounding myocardium. It is located on the basal portion of interventricular septum, and extends between the right atrium and ventricle.

## Validation study

Utilization of the cardiac atlas improved contour accuracy for all structures using both percent overlap and the concordance index (Figure 3). After application of the atlas, the heart and left ventricle achieved 91% and 92% overlap with the gold standard, respectively (Table 1). For small structures not frequently contoured in clinical practice, such as the left main coronary artery and right coronary artery, the percent overlap doubled after application of the atlas, although the absolute percentage was still relatively low. The concordance index score also improved significantly for all structures (Table 2). The highest concordances were found for the whole heart and ventricles. For the whole heart, concordance increased from  $0.76 \pm 0.11$  pre- to  $0.89 \pm 0.03$  post-atlas ( $p < 0.001$ ).

Following the placement of radiation fields, dosimetric analysis indicated a significant improvement in the consistency of dose reporting for several structures, including the heart, left main coronary artery, LAD, right coronary artery, and right ventricle (Table 3). The difference between the mean observer dose and gold standard dose for the heart improved from 0.9 Gy pre-atlas to 0.1 Gy post-atlas ( $p < 0.001$ ). Reported left main coronary artery and LAD dose improved from a difference of 1.7 Gy to 0.9 Gy ( $p = 0.005$ ), and 3.9 Gy to 2.6 Gy ( $p < 0.001$ ), respectively. Right ventricle dose also significantly improved, from a 1.1 Gy to 0.5 Gy ( $p = 0.008$ ) difference. There was no difference between the contrast and non-contrast scans in any metric we assessed.

## DISCUSSION

In the past few years, cardiac toxicity following radiotherapy for breast cancer has been recognized as an important issue. In the meta-analysis by the Early Breast Cancer Trialists' Collaborative Group including 78 randomized trials, an excess risk of mortality from heart disease (rate ratio 1.27) was found in patients who received adjuvant radiotherapy.<sup>4</sup> Hoening et al studied the treatment-specific incidence of cardiovascular disease in 4414 patients in the Dutch Late Effects Breast Cancer Cohort who had survived 10 years after treatment.<sup>1</sup> As compared to the incidence in the total Dutch female population, they found that patients who received radiation to the internal mammary nodes as part of their treatment had an increased risk of myocardial infarction (HR 1.7), congestive heart failure (HR 2.7), and valvular dysfunction (HR 3.2)

Harris et al reported a retrospective review of 961 patients with stages I and II breast cancer who received radiotherapy between 1977 and 1994 at the University of Pennsylvania.<sup>2</sup> With a median follow up of 12 years, they found that 20 years after treatment, patients who received left-sided radiotherapy had higher rates of coronary artery disease (25% vs. 10%), MI (15% vs. 5%), and cardiac deaths (6.4% vs. 3.6%) than patients who received right-sided radiotherapy.

Jagsi et al examined the University of Michigan experience of over 800 stage I or II breast cancer patients treated with radiotherapy between 1984 and 2000 and compared rates of cardiac events between patients treated to the left and right side. On multivariate analysis, the side of the treated breast did significantly predict for cardiac events, as might be expected, as the dose to heart structures is usually higher for patients with left- as compared to right-sided breast cancer.<sup>3</sup>

Most studies demonstrating an association of breast radiotherapy with cardiac morbidity are registry-based retrospective reviews, which depend on diagnosis codes and thus symptomatic cardiac toxicity. While these analyses provide some indication of radiation-associated morbidity and mortality, due to their retrospective nature, they may underestimate the true rates of cardiac damage. Prospective studies have been conducted to assess new

cardiac perfusion defects in asymptomatic patients following radiation exposure. While new defects have not yet been clearly correlated with cardiac morbidity or mortality, they appear to be a consequence of cardiac exposure to radiation. In a study of 294 patients who previously received at least 35 Gy of mediastinal radiation for Hodgkin's disease and had no known cardiac disease, 21% had abnormal ventricular images at rest on stress echocardiography and radionuclide perfusion imaging, indicating prior myocardial injury. An additional 14% developed perfusion defects during stress testing.<sup>5</sup> In another study of 114 patients treated with radiotherapy for left-sided breast cancer, perfusion defects seen in resting-gated single-photon emission computed tomography cardiac perfusion scans increased with time since completion of radiotherapy, so that over 40% of patients developed a new defect by 2 years. Over 25% of these defects were associated with wall-motion abnormalities. Importantly, there was a correlation between these abnormalities and the fraction of the left ventricle in the radiation fields.<sup>6</sup> These two studies illustrate a potentially high rate of cardiac damage associated with radiotherapy.

After breast radiotherapy, the early focus has been on ischemic cardiac disease, and since the LAD is the closest major coronary vessel to tangential breast fields, it stands to reason that it may be most often affected. Correa et al retrospectively examined the results of cardiac stress tests and catheterizations on patients who were treated with breast radiotherapy at the University of Pennsylvania between 1977 and 1994 and subsequently developed cardiac symptoms. They found a higher percentage of stress test abnormalities in patients who received left rather than right-sided radiotherapy (59% vs. 8%). 70% of the abnormalities were in the left anterior descending artery (LAD) territory. Catheterization confirmed the majority of coronary stenoses to be in the LAD.<sup>7</sup>

Although many studies regarding the cardiac toxicity of breast cancer have focused on ischemic disease, the detrimental effects of radiation on other cardiac structures such as the pericardium, myocardium, valves, conduction system, and autonomic system have also been described (Table 4)<sup>8</sup>.

Valvular dysfunction (regurgitation more often than stenosis) has been associated with mediastinal irradiation for malignancies such as Hodgkin's disease.<sup>9, 10</sup> In a Veteran's Administration study of 294 asymptomatic patients who had received at least 35 Gy of mediastinal irradiation and underwent electrocardiography and transthoracic echocardiography, the incidence of valvular disease increased with time since irradiation, with 60% of patients treated more than 20 years prior found to have mild or greater aortic regurgitation compared with only 4% of those treated within the past 10 years.<sup>9</sup> Diastolic dysfunction also has been described, presumably secondary to myocardial fibrosis.<sup>11</sup> Conduction system disruption is relatively rare, but can manifest as a bundle branch block or complete AV block.<sup>12-14</sup> Autopsy studies have found significant fibrosis of the conduction systems, out of proportion to the amount of fibrosis that can be attributed to coronary artery disease alone.<sup>12</sup>

Despite the known associations of radiation with long-term cardiac effects, no consistent dose-volume correlations have been found. This is likely due to the lack of detailed dosimetric studies with consistent cardiac substructure volume delineation. In this study, we created and validated an atlas which may be used in future efforts to determine such correlations, which can ultimately serve to set standard dosimetric limits to the heart. Initial data can be gathered not only from patients treated with radiotherapy for breast cancer, but also for any thoracic malignancy including lung cancer and lymphoma.

Application of the atlas improved contour accuracy in all structures, as measured by percent overlap of observer and gold standard volumes and the concordance index. Post-atlas



delineation of the whole heart and left ventricle volumes overlapped by more than 90%. However, despite a statistically significant greater than 2-fold improvement, the absolute percent overlap and concordance index for the right and left main coronary artery volumes remained quite low, at 24%, 0.18, 22%, and 0.18, respectively. This is likely due to the small structure volumes (1-2cc), which magnify the relative discrepancies in contours. In the recent RTOG breast cancer radiotherapy contouring study, their reported concordance index (referred to as percent overlap in their paper) was approximately 50% for the internal mammary nodes, which are also small structures (3.2cc in their 2 cases targeting these nodes).<sup>15</sup>

Dosimetric analysis indicated that the observed improvement in contour accuracy resulted in improved dose-reporting accuracy for the whole heart, left main coronary artery, LAD, right coronary artery, and right ventricle. The lack of improvement in dose-reporting for the left ventricle likely is a result of excellent pre-atlas agreement within 0.25 Gy of the gold standard, so that a post-atlas improvement to within 0.15 of the gold standard was not statistically significant ( $p=0.13$ ). Despite the relatively low percent overlap and concordance index for the left main and right coronary arteries noted above, dose reporting was quite accurate, within 0.9 and 0.6 Gy of the gold standard, respectively. This is likely due to the relatively low doses and gradual dose gradients that are seen near these structures with 3-dimensional breast radiation fields. It is possible that if applied to treatment plans for intrathoracic malignancies, or intensity-modulated radiotherapy plans, dose-reporting accuracy could improve for all, or a different combination of structures, depending on the location of the targets and the steepness of dose fall-off. Use of intravenous contrast did not improve contour accuracy or dose reporting, which is reassuring, since many centers do not routinely administer this for simulation scans. However, caution must be used if extrapolating to images obtained using older CT scanners, since the image quality may not be ideal.

This study serves as the first step toward gaining a deeper understanding of radiation effects on the heart. Correa et al examined potential predictive factors for developing cardiac disease after left-sided RT. However, the dosimetric factors considered were rudimentary and consisted of central lung distance and maximum heart width and length in the tangential radiation beams. No dose-volume parameters were studied.<sup>16</sup> In 1996, Gagliardi, et al determined a dose response curve for the heart and myocardium, based mainly on 3D reconstruction of 2D treatment plans, so the resulting dose-volume histograms on which the model was based, were not likely very accurate.<sup>17</sup>

Formal normal tissue complication probability models have been constructed for many organs including lung and liver for use in thoracic and abdominal tumor treatment planning, and formal dose-volume relationships have been recently also been derived for the parotid and submandibular glands and pharyngeal constrictors in head and neck radiotherapy.<sup>18-21</sup> With such information, treatment can be planned to stay below dose-volume parameters which may be expected to cause toxicity. Using consistent structure delineation, and therefore consistent dose reporting, we should be able to determine similar relationships for cardiac substructures and start to incorporate them into treatment planning.

Atlases have been developed in several disease sites in order to standardize target delineation. Examples include head and neck, prostate, rectal, and gynecologic malignancies, all developed through the RTOG. Earlier this year, the RTOG also finalized a breast radiotherapy atlas. However, organ at risk delineation is also important. The RTOG finalized a brachial plexus atlas this year. In the RTOG breast atlas, the whole heart is included, but it is likely that cardiac substructures are also important as we begin to understand the effects of radiotherapy on cardiac function. Thus, we have devised and

validated a more detailed atlas, which can also be used assessing the toxicity of radiotherapy for any thoracic malignancy.

Although a strong first step, there are limitations to the direct application of our atlas to clinical practice. Our CT images were not obtained using cardiac-gating, so structure contours were likely slightly blurred due to motion. The overall magnitude of this is small, but relatively more pronounced for small structures such as the left main coronary artery. The atlas was developed using respiratory-gated CT images to eliminate the major motion component, but respiratory-gating may not be routinely used in most centers for breast radiotherapy planning or treatment, although it is more often used for lung cancer. To most accurately assess dose to cardiac substructures, either treatment must be delivered in a single breath hold state, or we must have complete temporal-spatial information on these substructures to account for varying positions relative to isodose lines.

## CONCLUSION

We have developed a cardiac atlas and validated its effectiveness in improving the accuracy and concordance of contours, which led to improved dose reporting accuracy. This atlas can be applied not only to breast cancer treatment, but also any treatment which could potentially deliver radiation to a portion of the heart. Using consistent guidelines for structure delineation, we can begin to understand any causative effects of radiotherapy on cardiac morbidity and mortality with the goal of minimizing these risks in the future with multi-institutional clinical trials which include dose volume constraints on the heart and its substructures.

## Acknowledgments

Supported by NIH CA 102435

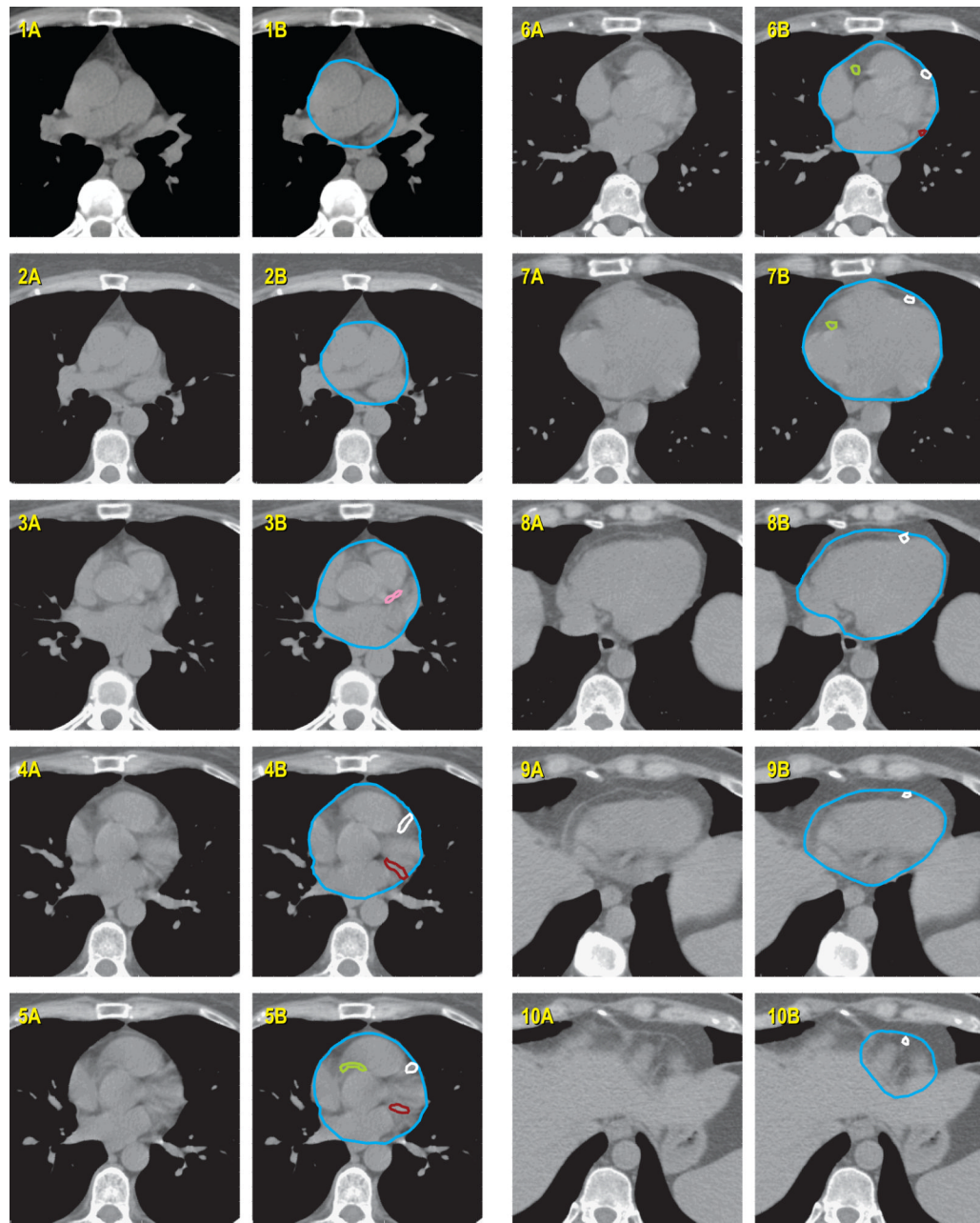
The authors would like to thank Steven Kronenberg for assistance with figures; and Karen Vineberg, Daniel Tatro, and Kathryn Masi for contour management and dosimetric assistance.

## References

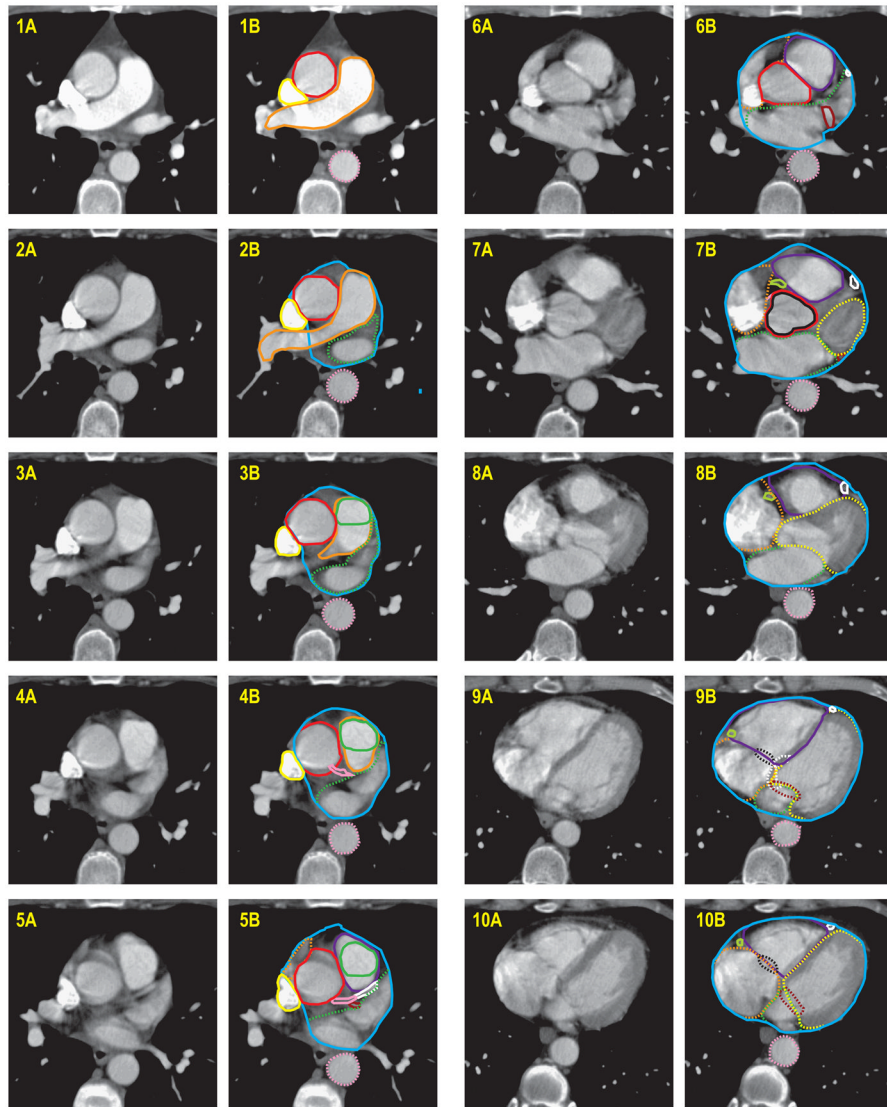
1. Hooning MJ, Botma A, Aleman BM, et al. Long-term risk of cardiovascular disease in 10-year survivors of breast cancer. *J Natl Cancer Inst* 2007;99:365–375. [PubMed: 17341728]
2. Harris EE, Correa C, Hwang WT, et al. Late cardiac mortality and morbidity in early-stage breast cancer patients after breast-conservation treatment. *J Clin Oncol* 2006;24:4100–4106. [PubMed: 16908933]
3. Jagsi R, Griffith KA, Koelling T, et al. Rates of myocardial infarction and coronary artery disease and risk factors in patients treated with radiation therapy for early-stage breast cancer. *Cancer* 2007;109:650–657. [PubMed: 17238178]
4. Clarke M, Collins R, Darby S, et al. Effects of radiotherapy and of differences in the extent of surgery for early breast cancer on local recurrence and 15-year survival: an overview of the randomised trials. *Lancet* 2005;366:2087–2106. [PubMed: 16360786]
5. Heidenreich PA, Schnittger I, Strauss HW, et al. Screening for coronary artery disease after mediastinal irradiation for Hodgkin's disease. *J Clin Oncol* 2007;25:43–49. [PubMed: 17194904]
6. Marks LB, Yu X, Prosnitz RG, et al. The incidence and functional consequences of RT-associated cardiac perfusion defects. *Int J Radiat Oncol Biol Phys* 2005;63:214–223. [PubMed: 16111592]
7. Correa CR, Litt HI, Hwang WT, et al. Coronary artery findings after left-sided compared with right-sided radiation treatment for early-stage breast cancer. *J Clin Oncol* 2007;25:3031–3037. [PubMed: 17634481]



8. Carver JR, Shapiro CL, Ng A, et al. American Society of Clinical Oncology clinical evidence review on the ongoing care of adult cancer survivors: cardiac and pulmonary late effects. *J Clin Oncol* 2007;25:3991–4008. [PubMed: 17577017]
9. Heidenreich PA, Hancock SL, Lee BK, et al. Asymptomatic cardiac disease following mediastinal irradiation. *J Am Coll Cardiol* 2003;42:743–749. [PubMed: 12932613]
10. Adabag AS, Dykoski R, Ward H, et al. Critical stenosis of aortic and mitral valves after mediastinal irradiation. *Catheter Cardiovasc Interv* 2004;63:247–250. [PubMed: 15390239]
11. Heidenreich PA, Hancock SL, Vagelos RH, et al. Diastolic dysfunction after mediastinal irradiation. *Am Heart J* 2005;150:977–982. [PubMed: 16290974]
12. Kaplan BM, Miller AJ, Bharati S, et al. Complete AV block following mediastinal radiation therapy: electrocardiographic and pathologic correlation and review of the world literature. *J Interv Card Electrophysiol* 1997;1:175–188. [PubMed: 9869969]
13. Mukerji S, Patel R, Khasnis A, et al. Recurrent syncope following radiation therapy. *Am J Med Sci* 2006;331:325–328. [PubMed: 16775441]
14. Tsagalou EP, Kanakakis J, Anastasiou-Nana MI. Complete heart block after mediastinal irradiation in a patient with the Wolff-Parkinson-White syndrome. *Int J Cardiol* 2005;104:108–110. [PubMed: 16137521]
15. Li XA, Tai A, Arthur DW, et al. Variability of target and normal structure delineation for breast cancer radiotherapy: an RTOG Multi-Institutional and Multiobserver Study. *Int J Radiat Oncol Biol Phys* 2009;73:944–951. [PubMed: 19215827]
16. Correa CR, Das IJ, Litt HI, et al. Association between tangential beam treatment parameters and cardiac abnormalities after definitive radiation treatment for left-sided breast cancer. *Int J Radiat Oncol Biol Phys* 2008;72:508–516. [PubMed: 18339489]
17. Gagliardi G, Lax I, Ottolenghi A, et al. Long-term cardiac mortality after radiotherapy of breast cancer—application of the relative seriality model. *Br J Radiol* 1996;69:839–846. [PubMed: 8983588]
18. Eisbruch A, Ten Haken RK, Kim HM, et al. Dose, volume, and function relationships in parotid salivary glands following conformal and intensity-modulated irradiation of head and neck cancer. *Int J Radiat Oncol Biol Phys* 1999;45:577–587. [PubMed: 10524409]
19. Feng FY, Kim HM, Lyden TH, et al. Intensity-modulated radiotherapy of head and neck cancer aiming to reduce dysphagia: early dose-effect relationships for the swallowing structures. *Int J Radiat Oncol Biol Phys* 2007;68:1289–1298. [PubMed: 17560051]
20. Lin A, Kim HM, Terrell JE, et al. Quality of life after parotid-sparing IMRT for head- and-neck cancer: a prospective longitudinal study. *Int J Radiat Oncol Biol Phys* 2003;57:61–70. [PubMed: 12909216]
21. Murdoch-Kinch CA, Kim HM, Vineberg KA, et al. Dose-effect relationships for the submandibular salivary glands and implications for their sparing by intensity modulated radiotherapy. *Int J Radiat Oncol Biol Phys* 2008;72:373–382. [PubMed: 18337023]



**Figure 1.** Cardiac atlas, without intravenous contrast. Contours are illustrated in the right column, with unmarked images provided in left column for reference. The key for figures 1 and 2 are the same.



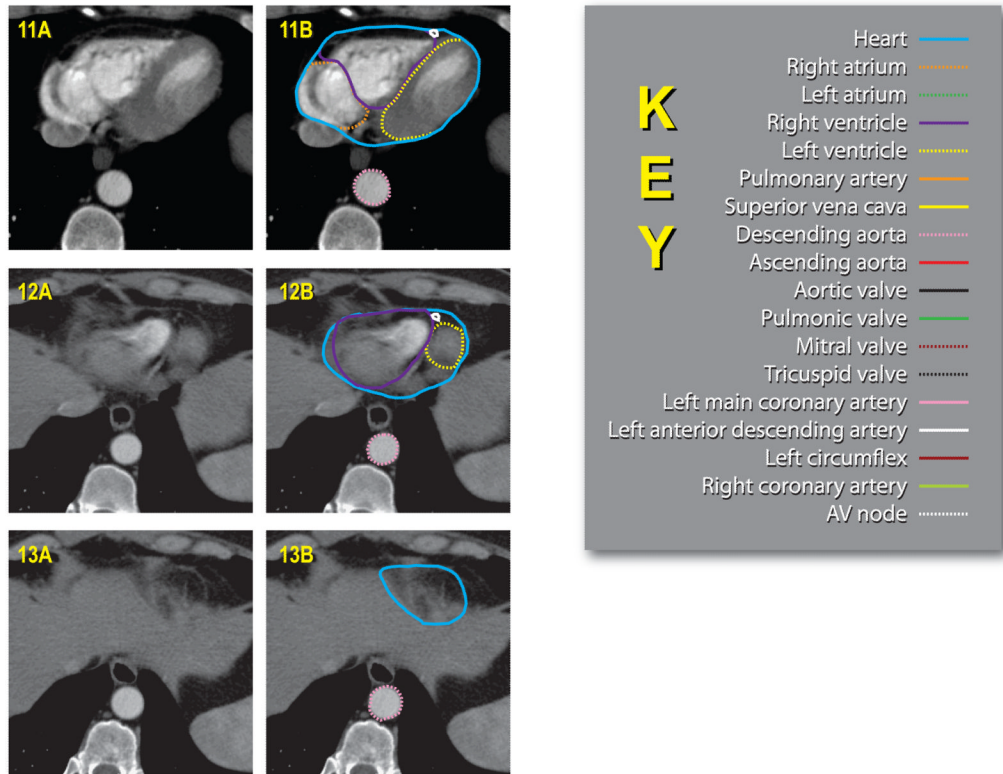


**Figure 2.** Cardiac atlas, with intravenous contrast. Contours are illustrated in the right column, with unmarked images provided in left column for reference.



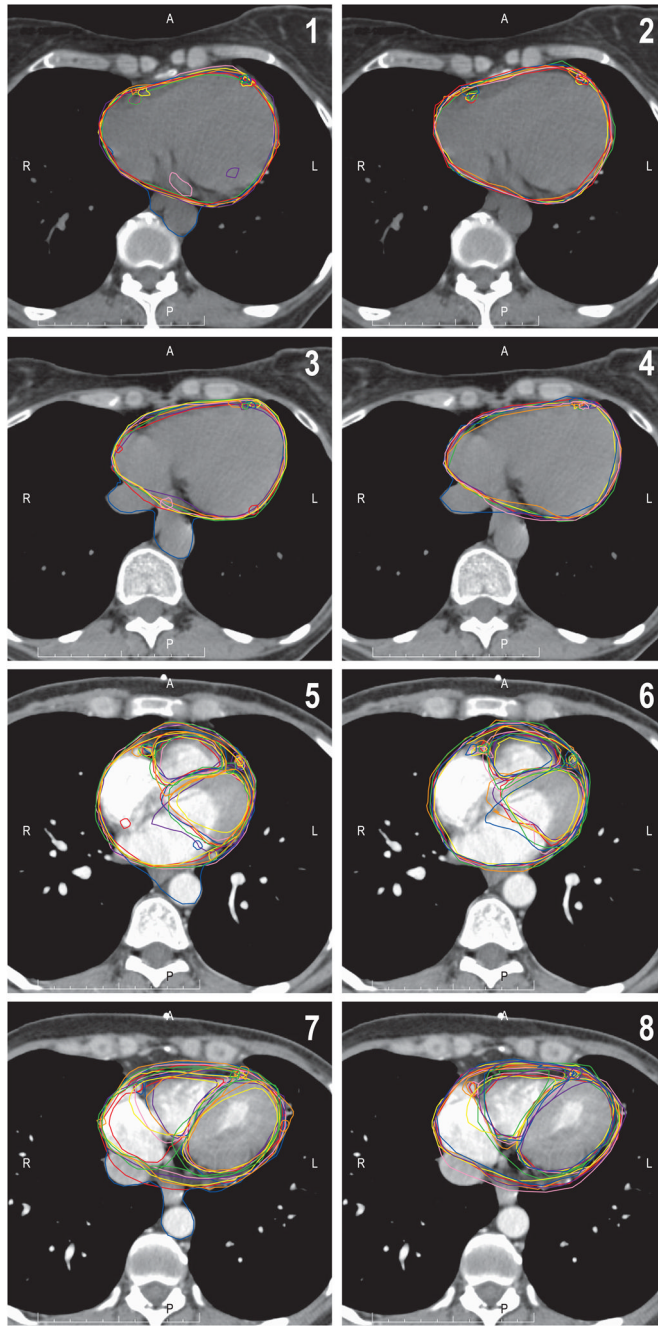


**Figure 3.** Improvement in cardiac substructure delineation consistency with the use of the cardiac atlas. Panels 1 and 3 show pre-atlas contours of 7 observers on 2 representative cardiac slices without intravenous contrast. The whole heart, right coronary artery, and left anterior descending coronary artery are displayed. Panels 2 and 4 show post-atlas contours on the same cardiac slices. Panels 5–8 show representative slices with intravenous contrast. The whole heart, right coronary artery, left anterior descending coronary artery, and right and left ventricles are displayed. Panels 5 and 7 are pre-atlas, and 6 and 8 are post-atlas. Notice the improvement in consistency, especially in cardiac vessel delineation.

**Table 1**  
**Percent overlap of observer and gold standard contours**

(mean  $\pm$ SD)

Structure	Pre-atlas (mean $\pm$ SD, range)	Post-atlas (mean $\pm$ SD, range)	p-value
Heart	79 $\pm$ 13 (50–99)	91 $\pm$ 4 (73–99)	<0.001
Left main coronary artery	10 $\pm$ 22 (0–72)	22 $\pm$ 20 (0–67)	<0.001
LAD*	35 $\pm$ 21 (0–77)	62 $\pm$ 16 (28–89)	<0.001
Right coronary artery	11 $\pm$ 14 (0–49)	24 $\pm$ 18 (0.2–59)	0.002
Left ventricle	87 $\pm$ 11 (62–99)	92 $\pm$ 6 (79–99)	0.06
Right ventricle	65 $\pm$ 10 (55–80)	74 $\pm$ 8 (61–88)	0.003

\* Left anterior descending coronary artery



**Table 2**  
**Concordance index**

(mean  $\pm$ SD)

Structure	Pre-atlas (mean $\pm$ SD, range)	Post-atlas (mean $\pm$ SD, range)	p-value
Heart	0.76 $\pm$ 0.11 (0.47–0.90)	0.89 $\pm$ 0.03 (0.72–0.94)	<0.001
Left main coronary artery	0.05 $\pm$ 0.12 (0–0.50)	0.18 $\pm$ 0.16 (0.01–0.50)	<0.001
LAD*	0.19 $\pm$ 0.11 (0–0.46)	0.34 $\pm$ 0.07 (0.30–0.47)	<0.001
Right coronary artery	0.08 $\pm$ 0.10 (0–0.32)	0.18 $\pm$ 0.08 (0.03–0.39)	<0.001
Left ventricle	0.75 $\pm$ 0.06 (0.62–0.84)	0.79 $\pm$ 0.05 (0.71–0.86)	0.04
Right ventricle	0.55 $\pm$ 0.08 (0.43–0.68)	0.65 $\pm$ 0.08 (0.55–0.78)	<0.001

\* Left anterior descending coronary artery

**Table 3****Mean Absolute Value**

[Observer contour dose – gold standard dose], Gy

	Pre-atlas (mean ± SD)	Post-atlas (mean ± SD)	p-value
Heart	0.88 ± 0.15	0.14 ± 0.14	<0.001
Left main coronary artery	1.68 ± 1.53	0.88 ± 1.56	0.005
LAD*	3.90 ± 2.80	2.56 ± 3.31	<0.001
Right coronary artery	1.15 ± 1.07	0.61 ± 0.39	0.001
Left ventricle	0.25 ± 0.20	0.15 ± 0.14	0.13
Right ventricle	1.06 ± 0.73	0.46 ± 0.37	0.008

\* Left anterior descending coronary artery

**Table 4**

## Spectrum of Radiation Damage to the Heart

Structure	Abnormality	Natural History	Pathology
Pericardium	Pericarditis	Chronic asymptomatic effusion and/or pericarditis with symptoms: hemodynamic compromise with either constriction or tamponade	Fibrous thickening and fluid production
Myocardium	Myocarditis	Progressive diastolic dysfunction and restrictive hemodynamics with symptoms: CHF	Diffuse interstitial fibrosis/ microcirculatory damage leading to capillary obstruction/extensive fibrosis
Endocardium	Valvular damage	Over time, progressive stenosis and regurgitation	Cusp and/or leaflet fibrosis
Vascular System	Arteritis	Premature CAD/accelerated atherosclerosis Pulmonary hypertension	Ostial and proximal stenosis; LAD, RCA, and left main more than left circumflex Pathology similar to atherosclerosis
Conduction System		All forms of heart block and conduction delay	Fibrosis of conduction system
Autonomic Dysfunction		Supraventricular tachycardia; heart rate variability	

\* Table from Carver et al, JCO 2007,(Carver, Shapiro et al. 2007) Reprinted with permission. © 2008 American Society of Clinical Oncology. All rights reserved.

\*\* CHF, congestive heart failure; CAD, coronary artery disease; LAD, left anterior descending [coronary artery]; RCA, right coronary artery.